Piezoelectric Energy Harvesting from Flow Induced Vibrations

D.-A. Wang, H.-H. Ko

Institute of Precision Engineering, National Chung Hsing University, Taichung 402, Taiwan, ROC

November 27, 2009

Abstract

A new piezoelectric energy harvester for harnessing energy from flow induced vibration is developed. It converts flow energy into electrical energy by piezoelectric conversion with oscillation of a piezoelectric film. A finite element model is developed in order to estimate the generated voltage of the piezoelectric laminate subjected to a distributed load. Prototypes of the energy harvester are fabricated and tested. Experimental results show that an open circuit output voltage of 2.2 V_{pp} and an instantaneous output power of 0.2 μW are generated when the excitation pressure oscillates with an amplitude of 1.196 kPa and a frequency of about 26 Hz. The solution of the generated voltage based on the finite element model agrees well with the experiments. Based on the finite element model, the effects of the piezoelectric film dimensions, the fluid pressure applied to the harvester and types of piezoelectric layer on the output voltage of the harvester can be investigated.

Keywords: Piezoelectric; Energy harvester; Finite element analysis

* Corresponding author. Tel.:+886-4-22840531; fax:+886-4-22858362

E-mail address: daw@dragon.nchu.edu.tw (D.-A. Wang).

1. Introduction

In recent years a considerable effort was focused on use of improved piezoelectric devices in the development of energy harvesters or micropower generators. By scavenging energy from the environment, miniature sensing/actuating devices can be self-powered in order to avoid the replacement of finite power sources. The development of microsystems located in harsh environment further demands for low power consumption and almost no maintenance requirement.

One approach to harvest energy is to convert mechanical energy of ambient vibration into electrical energy by piezoelectric devices. Piezoelectric harvesters have been proposed and investigated by many researchers, for example, see [1-10]. Allen and Smits [1] demonstrated the feasibility of an energy harvesting device based on the induced oscillation of a piezoelectric membrane placed behind the von Kármán vortex street formed behind a bluff body. Starner [2] analyzed the power generation of a piezoelectric film inserted in a shoe through leg motion. White et al. [3] constructed a piezoelectric energy harvester capable of generating a power of 2 μW. The cantilever beam structure of their device is tapered to obtain a constant strain along the length. Fang et al. [4] investigated a composite cantilever with a piezoelectric film sandwiched between metal electrodes. Under a vibration frequency of 608 Hz, the power output and the generated peak-to-peak voltage of their device are 2.16 μW and 890 mV, respectively. Lu et al. [5] described a piezoelectric laminated beam generator by bonding the piezoelectric element to a substructure undergoing bending. Guigon et al. [6] presented an experimental device that scavenges vibration energy from a piezoelectric flexible structure impacted by a water drop. Their device can provide a power output of

73 μW for the impact at 4.5 m/sec of a 3 mm diameter drop. Wang [7] developed piezoelectric nanogenerators using aligned nanowires for converting hydraulic and mechanical energy into electric energy. Zheng and Xu [8] reported two-beam cantilevers for vibration energy harvesting, where the top beam is a piezoelectric sheet and the bottom beam is an aluminum layer. Wacharasindhu and Kwon [9] fabricated and tested a device which can harness energy from typing motion on a computer keyboard by utilizing a piezoelectric layer and a magnet. Lee et al. [10] developed a piezoelectric energy harvester which can provide an output voltage of 2.675 V_{PP} and an output power of 2.765 μW when it is excited in the 31 mode. AdaptivEnergy's piezoelectric energy harvester harnesses the vibrations in its installed environment to generate electricity from vibration [11].

It may be possible to harvest the mechanical energy from the motion of fluid. Sanchez-Sanz et al. [12] accessed the feasibility of using the unsteady forces generated by the Kármán street around a micro-prism in the laminar flow regime for energy harvesting. They presented design guidelines for their energy-harvesting devices, but fabrication and experiments of the proposed device are not shown in their work. Holmes et al. [13] reported an electromagnetic generator integrated with a microfabricated axial-flow microturbine. The power output of the fabricated microdevice can be as high as 1.1 mW per stator when operated at a rotation speed of 30000 rpm, but the fabrication processes for their prototype involve deep reactive ion etching, multilevel electroplating, SU8 processing and laser micromachining. Herrault et al. [14] presented a rotary electromagnetic generator to harvest the mechanical energy of an air-driven turbine. The fabrication of their device requires electroforming, magnet demagnetization and laser

machining. A maximum output power of 6.6 mW is attained, when their device is driven at a rotation speed of 392000 rpm by an air turbine. Allen and Smits [1] used a piezoelectric membrane placed behind the von Kármán vortex street formed behind a bluff body to harvest energy from fluid motion. They examined the response of the membrane to vortex shedding. The power output of the membrane is not presented. Taylor et al. [15] developed an eel structure of piezoelectric polymer to convert mechanical flow energy to electrical power. They have focused on characterization and optimization of the individual subsystems of the eel system with a generation and storage units in a wave tank. Design and deployment of the eel system need further investigation. Tang et al. [16] designed a flutter-mill to generate electricity by extracting energy from fluid flow. Their structure is similar to the eel systems of Allen and Smits [1] and Taylor et al. [15]. They investigate the energy transfer between the structure and the fluid flow through an analytical approach. These authors utilized the flow-induced vibrations of fluid-structure interaction system to extract energy from the surrounding fluid flow [17]. The eel structures of Allen and Smits [1], Taylor et al. [15] and Tang et al. [16] have the potential to generate power from milli-watts to many watts depending on system size and flow velocity, but a power-generating eel has not been demonstrated. The devices of Holmes et al. [13] and Herrault et al. [14] require elaborate techniques for fabrication of their stator-rotor subcomponents and high rotation speeds for efficient energy harvesting. A device with simpler structure design and ease of application may be needed to extract energy from fluid motion.

In this paper, we develop a new energy-harvesting device based on flow-induced vibrations. It is motivated by the works of Allen and Smits [1] and Taylor et al. [15],

where a piezoelectric membrane or “eel” is placed in the wake of a bluff body and oscillates due to the vortices shed from the bluff body. As illustrated in Fig. 1, a flow channel with a flexible diaphragm is connected to a flow source. The pressure in the chamber causes the diaphragm to deflect in the upward direction. As the pressure increases to the maximum, the diaphragm reaches its highest position. When the pressure drops, the diaphragm moves downward. As the pressure decreases to the minimum, the diaphragm reaches its lowest position. Thus, by connecting the energy harvester to an ambient flow source, which is capable of providing the pressure change in the pressure chamber, the oscillating movement of the diaphragm with the piezoelectric film attached to it makes the energy harvesting possible. The focus of this paper is on the investigation of energy extraction from diaphragm vibration induced by a fluid flowing in a channel. In order to access the feasibility of the proposed energy harvester, finite element analyses are carried out to estimate the output voltage of the piezoelectric film. Fabrication of the energy harvester with a molding process and an assembly technique is described. Experimental setup used to measure the deflection and voltage output of the device is reported. The fabricated device is tested under its first resonance frequency. The experimental results are compared with the results of the analyses.

2. Design

2.1 Operational principle

Our design of the piezoelectric energy harvester is based on the vibration induced by liquid flow in channels. The variation of the liquid pressure in the channel drives a polydimethylsiloxane (PDMS) diaphragm and a piezoelectric film into vibration. The

vibration energy is converted to electrical energy by the piezoelectric film. A piezoelectric energy harvester is shown in Fig. 2(a). Fig. 2(b) is an exploded view of the energy harvester. It consists of a flow channel with two glass tubes, a PDMS diaphragm bonded to the channel, and a piezoelectric film glued to the PDMS diaphragm.

This harvesting of flow energy via a flow-induced vibration is related to the response of a flexible diaphragm to an internal flow. The flow is bounded by the flexible structure and rigid walls. If the diaphragm has small inertia and is flexible enough to be able to respond rapidly to the fluctuating pressure field set up by the flow, one may expect that the diaphragm may oscillate with a frequency similar to that observed in the flow. When the fluctuating pressure is applied on the surface of the diaphragm, the piezoelectric film strains laterally. The normal strain causes electrical charge to accumulate on the piezoelectric electrode, resulting in a voltage in the thickness direction of the piezoelectric film. For convenience of analysis, a simple model is developed to estimate the voltage generated in the piezoelectric film.

2.2 A model for estimation of the voltage generated in the piezoelectric film

Using Gauss's law, the charge accumulated on the piezoelectric electrodes is given by

$$Q = \oint_S D_3 dA \tag{1}$$

where D_3 is the electrical displacement in the thickness direction, and dA is a differential area on the electrode surface S. For the piezoelectric film mounted on the diaphragm as shown in Fig. 2(b), we have

$$D_3 = d_{31}\sigma_{xx} + d_{31}\sigma_{yy} + d_{33}\sigma_{zz} \tag{2}$$

where σ_{xx}, σ_{yy} and σ_{zz} are the normal stresses in the x, y and z direction, respectively. d_{31} and d_{33} are piezoelectric constants. The voltage generated in the piezoelectric film can be expressed as

$$V = \frac{Q}{C} \tag{3}$$

where C is the capacitance of the piezoelectric film.

Due to the asymmetric laminated structure of the device, finite element analyses are carried out to obtain the normal stresses in the piezoelectric film. The dimensions of the energy harvester are indicated in Fig. 2. A Cartesian coordinate system is shown in the figure. Due to symmetry, only a quarter model is considered. Fig. 3(a) shows a mesh for a finite element model. As shown in Fig. 3(a), the deflections in the x and y directions of the PDMS diaphragm at the circumference of the pressure chamber are constrained to represent the fixed boundary conditions. The lateral surfaces of the piezoelectric film are assumed to be free. The bottom surface of the piezoelectric film is rigidly connected to the top surface of the PDMS diaphragm. A pressure P is applied at the bottom surface of the diaphragm. The displacement in the x and y direction of the symmetry plane, the $y-z$ and $x-z$ plane, respectively, is constrained to represent the symmetry condition due to the loading conditions and the geometry of the device. Fig. 3(b) shows a close-up view of the mesh near the center of the diaphragm. The piezoelectric film (LDT0-028K/L, Measurement Specialties, Inc., US) is a laminated film including a polyvinylidene fluoride (PVDF) film, two silver electrode layers and a polyester (PE) layer. The PDMS diaphragm has a thickness of 200 μm. The electrode layers with a thickness of 28 μm are attached the top and bottom surfaces of the PVDF

film of 24 μm. A 125 μm PE layer is laminated to the top surface of the top electrode layer. When used in a bending mode, the laminated piezoelectric film develop much higher voltage output when flexed than a non-laminated film. The neutral axis is in the PE layer instead of in the PVDF film so the film is strained more when flexed. The finite element model has 625 20-node quadratic elements. A mesh convergence study is performed to obtain accurate solutions of charge accumulation.

The material properties of the PVDF film, the silver electrodes and the PE layer are listed in Table 1. The mechanical behavior of the PDMS diaphragm is described by the Marlow model in Abaqus for approximately incompressible isotropic elastomers [18], where the Marlow model is defined using the uniaxial tensile test data. Fig. 4 shows the measured engineering stress - engineering strain curve of the PDMS material. The PDMS material tested is cured at $80^{o}C$ for 40 minutes in an acrylic mold before cutting into the size of the tensile test specimens. The specimens are prepared following the ASTM D 882 test standard for thin plastic sheeting. To address the potential issues with PDMS aging, the tensile tests are performed within 36 hours after the curing of the PDMS material [19]. The aging occurs because of changes in internal structure due to curing or other processes [20]. The density of the PDMS material is taken as 1670 kg/m^3 by measuring the weight and volume of the fabricated PDMS. The commercial finite element program ABAQUS [18] is employed to perform the computations. 20-node piezoelectric element C3D20RE is used to model the PVDF film. The element type used for the PDMS diaphragm is the 20-node hybrid element C3D20RH.

2.3 Analysis

Fig. 5 shows the induced peak-to-peak voltage as a function of the pressure difference $P_{\max} - P_{\min}$ in the pressure chamber based on the finite element model. The values of the pressure loads considered are based on the measured pressures in the pressure chamber of a fabricated prototype. The peak-to-peak voltage increases nearly linearly as the pressure difference increases, since the behaviors of the materials are assumed to be linear elastic in the model. For the pressure difference ranging from 1.790 to 2.392 kPa, the maximum and minimum of the generated peak-to-peak voltage are 1.77 and 2.30 V, respectively. Based on the finite element computations, the ratio of magnitude between the stresses σ_{xx}, σ_{yy}, and σ_{zz} is nearly 4:20:1 for the loadings considered. The effect of σ_{zz}, through-thickness stress, is relatively small when compared to σ_{xx} and σ_{yy}, in-plane stresses.

The static analysis for the energy harvester can be used for low frequency applications. The model for estimation of the voltage generated in the piezoelectric film can be used for the feasibility study of the proposed energy harvesting device. For more accurate estimation of voltage generation, a dynamic analysis should be carried out.

3. Fabrication, experiments and discussions

3.1 Fabrication

In order to verify the effectiveness of the proposed energy harvesting device, prototypes of the energy harvester are fabricated. The PDMS flow channel is fabricated by a molding process in an acrylic mold. Fig. 6 shows the fabrication steps. First, an acrylic mold is carved by a milling machine (PNC-3100, Roland DGA Co., Japan). Next,

the PDMS material is poured over the mold to form the flow channel. The PDMS material is composed of two parts, a curing agent and the polymer. They are mixed with a volume ratio of 1:10. Before pouring into the mold, the mixture is degassed under vacuum until no bubbles appear. The PDMS is cured at $80^{o}C$ for 40 minutes. Then, the PDMS is peeled off from the mold.

Fig. 7 shows the assembly steps of the energy harvester. First, the inlet and outlet of the PDMS channel are prepared by piercing the front and back ends of the cured PDMS using a copper tube with an outer diameter of 2.5 mm. Subsequently, a PDMS diaphragm of 200 μm is glued to the flow channel by a thin layer of the liquid PDMS mixture. Two glass tubes are squeezed into the inlet and outlet hole, respectively. The inlet and outlet are permanently sealed by applying the PDMS mixture, which is cured at $80^{\circ}C$ for 90 minutes. As reported by Liu et al. [21], PDMS can seal to itself and/or to other flat surfaces with thermal heating promoted bonding process with a good watertight capability. Finally, the piezoelectric film is glued to the flow channel by applying an adhesive (3M Scotch) to complete the assembly steps. The thickness of the adhesive after the assembly step is nearly 50 μm. Fig. 8(a) and (b) are photos of a fabricated PDMS flow channel and an assembled energy harvester, respectively.

3.2 Experiments

Fig. 9 is a schematic of the experimental apparatus for testing of the fabricated device. The energy harvester is placed on the platform of a tank. Tap water is pumped into the inlet of the energy harvester through a pulse pump to provide a periodic pressure in the pressure chamber of the energy harvester. The oscillating deflection of the

piezoelectric film is measured by a Philtec D6 fiberoptic displacement sensor. The generated voltage of the PVDF film is amplified and filtered by a Stanford SR560 preamplifier and is recorded and analyzed by a data acquisition unit (PCI-5114, National Instruments Co., US). Fig. 10 is a photo of a close-up view of the experimental apparatus.

The experimental results are shown in Fig. 11. Fig. 11(a) shows the pressure history in the pressure chamber, where the mean pressure and the pressure difference $P_{\max} - P_{\min}$ within the pressure chamber is 2.473 and 2.392 kPa, respectively. The pressure is measured with a subminiature pressure sensor (PS-05KC, Kyowa Electronic Instruments Co. Ltd., Japan) embedded in the pressure chamber. The pressure sensor is connected to a data acquisition unit (DBU-120A, Kyowa Electronic Instruments Co. Ltd., Japan). The measured deflection history of the center of the piezoelectric film is shown in Fig. 11(b). The film oscillates around a deflected position of 367 μm with an amplitude about 188 μm. The measured open circuit voltage generated by the PVDF film is shown in Fig. 11(c). The output peak-to-peak voltage for an oscillation amplitude of 1.196 kPa and an excitation frequency of 26 Hz of the pressure in the pressure chamber is nearly 2.2 V. The experimental results do not show transient responses since they are recorded at steady state vibration. The open circuit voltage as a function of the pressure difference in the pressure chamber ranging from 1.790 to 2.392 kPa is shown in Fig. 5. The output voltage has a nearly linear relationship to the pressure difference and is in good agreement with the result based on the finite element model except that at the pressure difference of 2.392 kPa. The slightly lower output voltage at the pressure difference of 2.392 kPa can be attributed to the PDMS aging. It should be noted that the experimental results are obtained after one week of device fabrication. At higher stress

level, the material hardening effect of the polymer due to aging may be higher. The experimental values in the figure demonstrate that the model provides a relatively accurate prediction of the generated voltage. This indicates that the model can be effective as a design tool to determine the size and excitation pressure level necessary to provide the desired voltage output as far as the behavior of the materials of the piezoelectric laminate is linear elastic.

The fabricated device has been operated continuously for 4 hours at the rate of 93600 cycles/hr for an oscillation amplitude of 1.196 kPa and an excitation frequency of 26 Hz of the pressure in the pressure chamber. The device is run for a total of 152 hours without failure, accumulating a total of 14 million cycles. In order to evaluate the harvesting system, experiments on the electrical power output of the device are performed. A matched load can be connected to the device to maximize output power. The internal electrical resistance of the device is measured by a LCR meter (WK 4235, Wayne Kerr Electronics, Ltd., UK). The impedance of the probe is 200 kΩ. The measurement range is from 0 MΩ to 100 MΩ at a specified error of less than 1 % over the frequency band 10 Hz – 1 MHz. The instantaneous power can be expressed as

$$P = \frac{(\sqrt{2}\tilde{V})^2}{R} \tag{4}$$

where R is the resistance value of the matched load and $\tilde{V}$ is the root-mean-square value of the voltage drop across the matched load. By connecting the matched load of 10 MΩ to the device and detecting the voltage drop across the matched load, 0.708 V_{rms}, the instantaneous power is determined as 0.2 μW under an excitation frequency of 26 Hz and a pressure amplitude of 1.196 kPa in the pressure chamber.

Fig. 12 shows the deflection of the center of the piezoelectric film as a function of the excitation frequency based on the experiments. Due to the capability of the pulse pump for pumping water into the flow channel, the lowest excitation frequency which can be attained is 25.7 Hz. The measured resonance frequency of the device is 26 Hz, which is the excitation frequency used throughout the investigation. The resonance frequency based on a static finite element analysis is 159 Hz, where water in the flow channel is not modeled. Resonant frequencies are expected to shift in a water environment, since water affects the viscous damping of the structure and adds hydromass to it [22]. The hydromass of a circular disk near a rigid surface can be taken as [23]

$$m_f = \frac{\pi \rho a^4}{8G} \tag{5}$$

where a is the radius of the circular disk, G is the gap between the disk and the rigid surface, and ρ is the density of the fluid. The resonance frequency of the device with the contribution of the hydromass can be approximated as

$$\omega_f = \sqrt{\frac{m_s}{m_f + m_s}}\omega_s \tag{6}$$

where m_s and ω_s are the mass and resonance frequency of the structure, respectively. Using equations (5) and (6), the resonance frequency of the device is calculated as 37 Hz, where the density of the fluid, water, is taken as 1 g/cm^3, and a and G are 10 mm and 4 mm, respectively (as shown in Fig. 2(b)). The mass of the structure, m_s, is calculated as 0.055 g. The higher simulated result could be attributed to the neglected structural damping, air damping at the outside of the device and fabrication/assembly error.

In this investigation, the device is operated at its first resonance frequency. Most energy harvesting device based on piezoelectric effects have focused on single-frequency ambient energy, i.e. resonance-based energy harvesting [24]. When the ambient excitation is at a single frequency, the design of the energy harvesting device can be tailored to the ambient frequency available. For random and broadband ambient flow sources, the device may not be robust. To account for the variations in the excitation frequency, a device with an array of structures with various resonance frequencies can be utilized [25]. The other possible route to account for the random ambient flow sources is to minimize the mechanical damping or maximize the electromechanical coupling of the device [24]. A structure with multiple resonant frequencies may also be considered for energy harvesting from random vibrations with multiple resonant peaks, for example a segmented composite beam with embedded piezoelectric layers [26]. As shown in Fig. 12, the device is sensitive to frequency drift, it is not applicable where a single frequency ambient energy source is not available. In order to account for the frequency drift in the ambient energy source, new designs of the device must be investigated for its potential applications in power supply of remote wireless sensors.

In the analysis for voltage generation, the pressure within the chamber is assumed to be uniformly distributed. In order to verify this assumption, a two-dimensional flow analysis is carried out using a commercial software ANSYS FLOTRAN. In the analysis, a uniform velocity profile at the inlet along the direction of the inlet flow is applied. No-slip (zero velocity) conditions all along the channel walls are specified. The fluid is considered incompressible. It is assumed that only the relative value of pressure is important, and a zero pressure is applied at the outlet of the channel. The Reynolds

number is calculated in order to determine if the analysis is in the turbulent region. The Reynolds number of the flow channel can be determined by

$$\mathrm{Re} = \rho V D_h / \mu \tag{7}$$

where V is the flow velocity at the inlet of the diffuser element of the device, and μ is the dynamic viscosity of the water, 1.002×10^{-3} Pa $\cdot$ sec. D_h is the hydraulic diameter, which is taken as twice the inlet height, 8 mm. With the excitation frequency of 26 Hz, the measured values of V is 88.6 ± 1 cm/sec, and the calculated Re is nearly 7000, which is turbulent. Using the turbulent model of ANSYS FLOTRAN, the pressure distribution of the flow channel is obtained. The deviation of the pressure in the chamber along the symmetry axis is less than 4%, which is quite uniform.

In order to generate the pressure fluctuation in the channel, a pulse pump is used to pump tap water into the flow channel in the laboratory environment. Energy can be harvested from unsteady geophysical flows (ocean or river currents) or random fluctuation of tire pressure due to ambient temperature changes or contact between vehicle tire and pavement surface.

Compared to other researchers' work to extract energy from flow-induced vibrations of fluid-structure interaction system [1, 13-16], the presented design might be simpler in its structure and fabrication, since the devices of Holmes et al. [13] and Herrault et al. [14] consist of stator-rotor subcomponents, which need elaborate fabrication steps, and a high rotation speed may be needed for efficient energy harvesting. The eel structure of Allen and Smits [1] has proved to be feasible by simulation and hydrodynamic testing, but a power-generating eel is not demonstrated. Taylor et al. [15] have demonstrated an eel structure with a power generation and storage system in a wave

tank. The length, width and thickness of their eel are 9.5", 3", and 0.15 mm, respectively. The challenge to design and deploy a miniaturized eel-like system remains. Although the output power of our device is relatively low, given the structure design of the flow channel and the piezoelectric film, the dimensions of the device can be decreased for construction of a miniaturized system to harvest energy from flow motion by solid-fluid interaction.

4. Conclusions

A d31 mode piezoelectric energy harvester is developed. The energy is harvested from flow induced vibration. The pressure oscillation in the pressure chamber of the harvester results in a periodical deflection of the piezoelectric laminate and therefore the voltage generation. A finite element model of the output voltage of the device is developed for quick evaluation of the effects of device dimensions, pressure loads and material properties on the performance of the energy harvester. Prototypes of the energy harvester are fabricated and tested. The measurements conducted in various pressure difference in the pressure chamber of the device show that the maximum generated voltage and instantaneous power are approximately 2.2 V_{pp} and 0.2 μW, respectively, when the excitation pressure oscillates with an amplitude of 1.196 kPa and a frequency of about 26 Hz. The generated voltages based on the finite element model agree well with the experiments. The model can be used to predict the performance of the energy harvester with different dimensions, material properties and pressure loads.

Sources of flow induced vibration can be unsteady geophysical flows (ocean or river currents) or random fluctuation of tire pressure due to ambient temperature changes

or contact between vehicle tire and pavement surface. The periodic vortex shedding behind a blunt body immersed in a steady stream causes a pressure oscillation in the stream. This regular, periodic shedding can be integrated into the flow channel of the proposed device to scavenge the flow energy.

Acknowledgement

This work is financially supported by Precision Machinery Research and Development Center (Contract Number: 98TR10). Partial support of this work by a grant from National Science Council, Taiwan (Grant Number: NSC 96-2221-E-005-095) is greatly appreciated. The authors would like to express their appreciation to the National Center for High-Performance Computing (NCHC), Taiwan for their assistance. Helpful discussions with Professor Yuen-Wuu Suen of National Chung Hsing University, Taiwan, R.O.C. are greatly appreciated.

References

[1] J. J. Allen and A. J. Smits, Energy harvesting eel, Journal of Fluid and Structures, 15 (2001) 629-640.

[2] T. Starner, Human-powered wearable computing, IBM Systems Journal, 35 (1996) 618-629.

[3] N. M. White, P. Glynne-Jones and S. P. Beeby, A novel thick-film piezoelectric micro-generator, Smart Materials and Structures, 10 (2001) 850-852.

[4] H.-B. Fang, J.-Q. Liu, Z.-Y. Xu, L. Dong, L. Wang, D. Chen, B.-C. Cai, Y. Liu, Fabrication and performance of MEMS-based piezoelectric power generator for vibration energy harvesting, Microelectronics Journal, 37 (2006) 1280-1284.

[5] F. Lu, H. P. Lee and S. P. Lim, Modeling and analysis of micro piezoelectric power generators for micro-electromechanical-systems applications, Smart Materials and Structures, 13 (2004) 57-63.

[6] R. Guigon, J.-J. Chaillout, T. Jager and G. Despesse, Harvesting raindrop energy: experimental study, Smart Materials and Structures, 17 (2008) 015039.

[7] Z. L. Wang, Energy harvesting for self-powered nanosystems, Nano Research, 1 (2008) 1-8.

[8] Q. Zheng and Y. Xu, Asymmetric air-spaced cantilevers for vibration energy harvesting, Smart materials and Structures, 17 (2008) 055009.

[9] T. Wacharasindhu and J. W. Kwon, A micromachined energy harvester from a keyboard using combined electromagnetic and piezoelectric conversion, Journal of Micromechanics and Microengineering, 18 (2008) 104016.

[10] B. S. Lee, S. C. Lin, W. J. Wu, X. Y. Wang, P. Z. Chang, C. K. Lee, Piezoelectric MEMS generators fabricated with an aerosol deposition PZT thin film, Journal of Micromechanics and Microengineering, 19 (2009) 065014.

[11] R. Quinnell, Energy scavenging offers endless power possibilities, Electronic Design Europe, 07.05.09 (2009) 5-8.

[12] M. Sanchez-Sanz, B. Fernandez and A. Velazquez, Energy-harvesting microresonator based on the forces generated by the Kammon street around a rectangular prism, Journal of Microelectromechanical Systems, 18 (2009) 449-457.

[13] A. S. Holmes, G. Hong and K. P. Pullen, Axial-flux permanent magnet machines for

micropower generation, Journal of Microelectromechanical Systems, 14 (2005) 54-62.

[14] F. Herrault, C.-H. Ji and M. G. Allen, Ultraminiaturized high-speed permanent-magnet generators for milliwatt-level power generation, Journal of Microelectromechanical Systems, 17 (2008) 1376-1387.

[15] G. W. Taylor, J. R. Burns, S. M. Kammann, W. B. Powers and T. R. Welsh, The energy harvesting eel: A small subsurface ocean/river power generator, IEEE Journal of Oceanic Engineering, 26 (2001) 539-547.

[16] L. Tang, M. P. Païdoussis and J. Jiang, Cantilevered flexible plates in axial flow: Energy transfer and the concept of flutter-mill, Journal of Sound and Vibration, 326 (2009) 263-276.

[17] R. D. Blevins, Flow-induced vibration, 2nd edition, Van Nostrand Reinhold, New York, 1990.

[18] H. D. Hibbitt, B. I. Karlsson. E. P. Sorensen, *ABAQUS user manual*, Version 6-2, HKS Inc. Providence, RI, USA, 2001.

[19] D. N. Hohne, J. G. Younger, M. J. Solomon, Flexible microfluidic devices for mechanical property characterization of soft viscoelastic solids such as bacterial biofilms, Langmuir, 25 (2009) 7743-7751.

[20] A. S. Wineman and K. R. Rajagopal, Mechanical response of polymers, Cambridge University Press, Cambridge, UK, 2000.

[21] M. Liu, J. Sun and Q. Chen, Influences of heating temperature on mechanical properties of polydimethylsiloxane, *Sensors and Actuators A*, 151 (2009) 42-45.

[22] N. Piccirillo, Analysis of fluid-structural instability in water, Proc. SPIE Vol. 3089, Proceedings of the 15th International Modal Analysis Conference, pp. 343-349, 1997.

[23] R. J. Fritz, The effect of liquids on the dynamic motions of immersed solids, Transactions of ASME, Journal of Engineers for Industry 94 (1972) 167-173.

[24] S. Adhikari, M. I. Friswell and D. J. Inman, Piezoelectric energy harvesting from broadband random vibrations, Smart Materials and Structures, 18 (2009) 115005.

[25] J.-Q. Liu, H.-B. Fang, Z.-Y. Xu, X.-H. Mao, X.-C. Shen, D. Chen, H. Liao and B.-C. Cai, A MEMS-based piezoelectric power generator array for vibration energy

harvesting, Microelectronics Journal, 39 (2008) 802-806.

[26] S. Lee, B. D. Youn and B. C. Jung, Robust segment-type energy harvester and its application to a wireless sensor, Smart Materials and Structures, 18 (2009) 095021.

Biography

Dung-An Wang received the Ph.D. degree in mechanical engineering from the University of Michigan at Ann Arbor, in 2004. He is currently an Assistant Professor in the Institute of Precision Engineering, National Chung Hsing University, Taiwan, ROC. His research interests include micromachined resonators and actuators, piezoelectric actuators, microassembly and compliant mechanisms.

Hong-Hua Ko received the B.S. degree in mechanical and mechatronic engineering from the National Taiwan Ocean University, Taiwan, ROC, in 2007, and is currently working towards the M.S. degree in the Institute of Precision Engineering, National Chung Hsing University, Taiwan, ROC. His research interests are piezoelectric actuators, and microassembly.

Table 1. Properties of the PVDF film, the silver electrodes and the PE layer

	Property	Tensor (in order of *x*, *y*, *z*, *xy*, *xz*, *yz*)
PVDF film	Piezoelectricity **d** ($\mathrm{m \cdot V^{-1}}$)	$10^{-12} \times \begin{bmatrix} 0 & 0 & 23 \\ 0 & 0 & 23 \\ 0 & 0 & -33 \\ 0 & 0 & 0 \\ -27 & 0 & 0 \\ 0 & -23 & 0 \end{bmatrix}$
	Permittivity ε ($\mathrm{F \cdot m^{-1}}$)	$10^{-12} \times \begin{bmatrix} 110 & 0 & 0 \\ 0 & 110 & 0 \\ 0 & 0 & 110 \end{bmatrix}$
	Density ($\mathrm{kg \cdot m^{-3}}$)	1780
	Young's modulus (GPa)	3
	Poisson's ratio	0.35
	Capacitance ($\mathrm{pF \cdot cm^{-2}}$	380
Polyester layer	Density ($\mathrm{kg \cdot m^{-3}}$)	1300
	Young's modulus (GPa)	3.5
	Poisson's ratio	0.25
Silver electrode	Density ($\mathrm{kg \cdot m^{-3}}$)	10500
	Young's modulus (GPa)	83
	Poisson's ratio	0.37

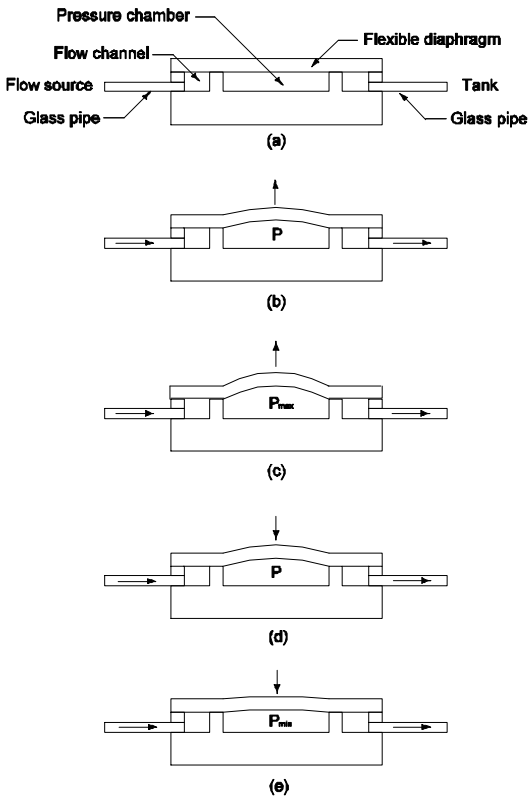

Fig. 1. Operation of a piezoelectric energy harvester.

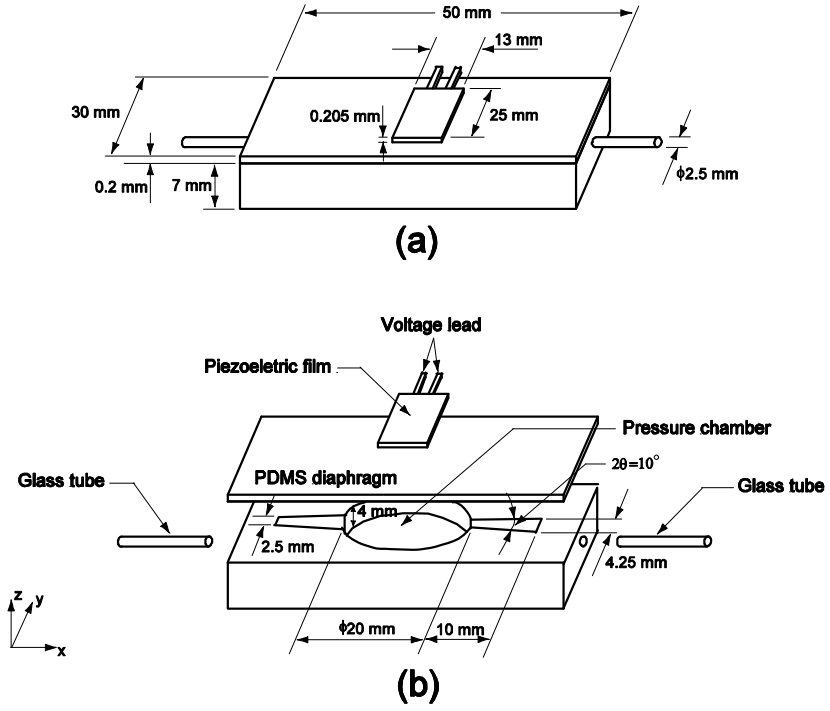

Fig. 2. (a) An assembled energy harvester. (b) Components of the energy harvester.

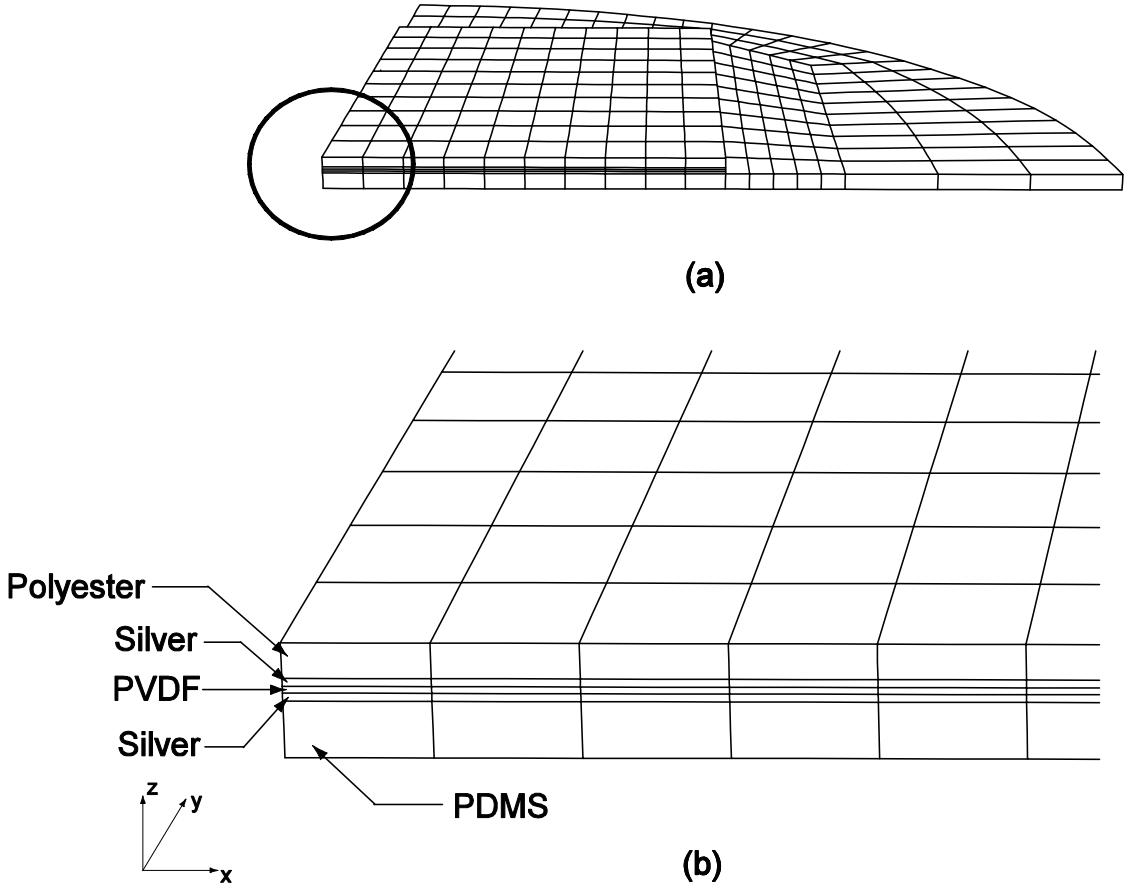

Fig. 3. (a) A finite element mesh of the PDMS diaphragm and the piezoelectric film. (b) A close-up view of the mesh near the center of the diaphragm.

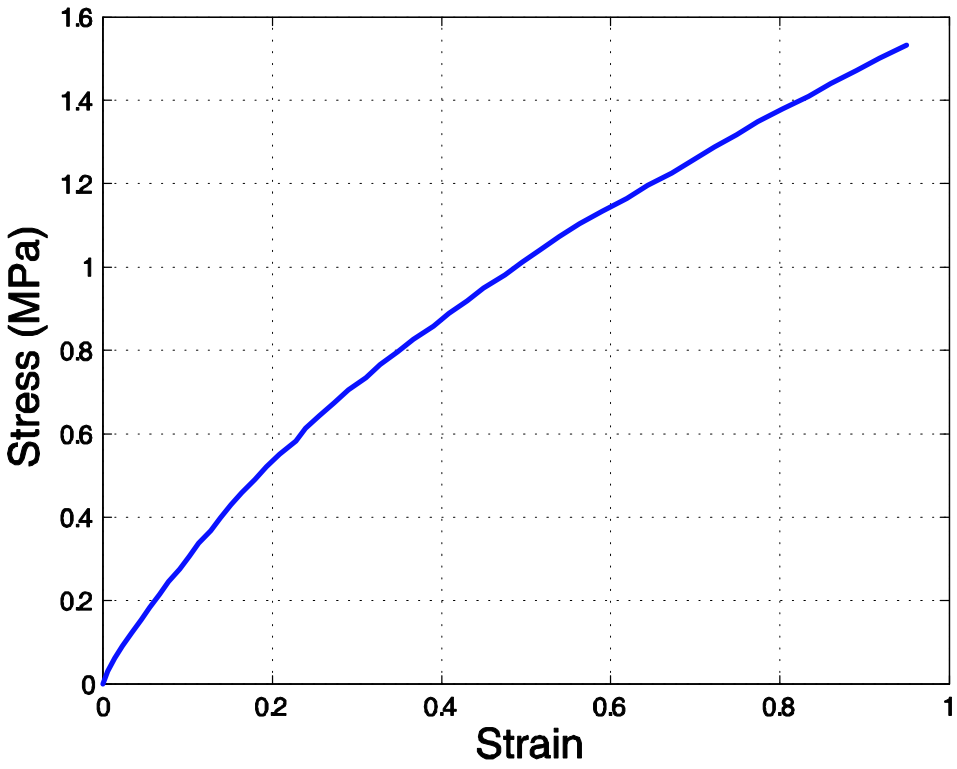

Fig. 4. Measured stress-strain curve of the PDMS material.

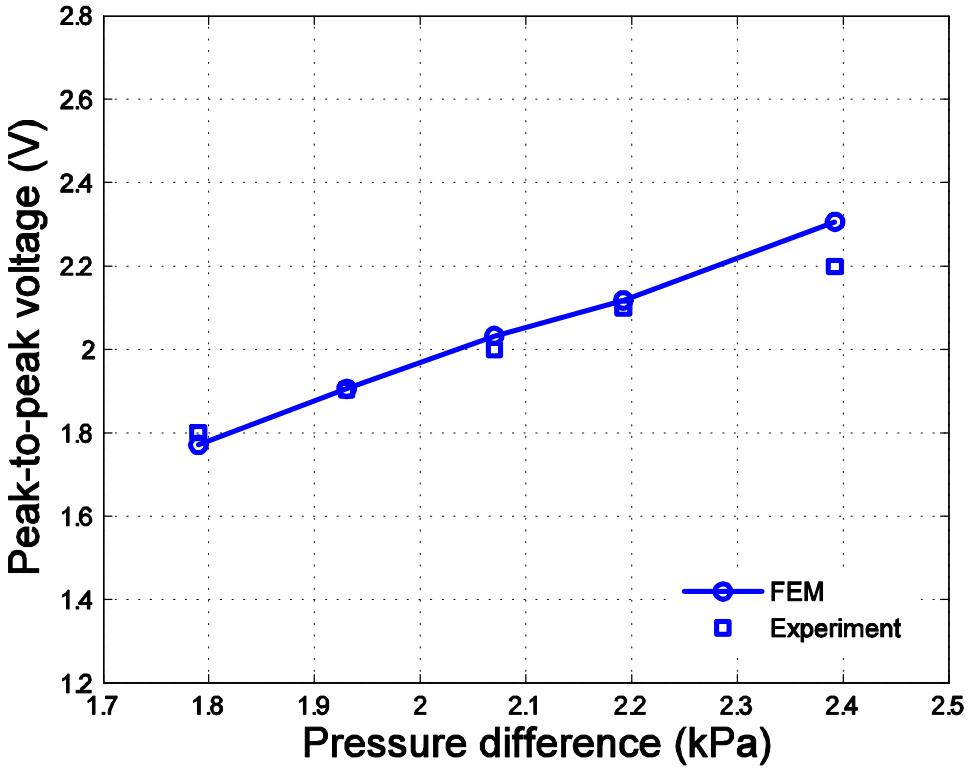

Fig. 5. Generated peak-to-peak voltage as a function of the pressure difference in the pressure chamber.

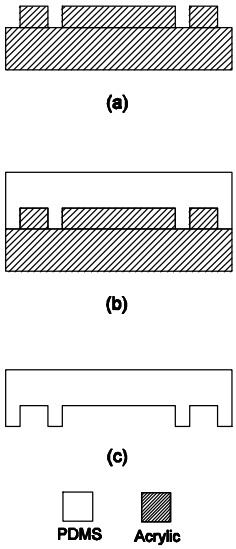

Fig. 6. Fabrication steps of the PDMS channel.

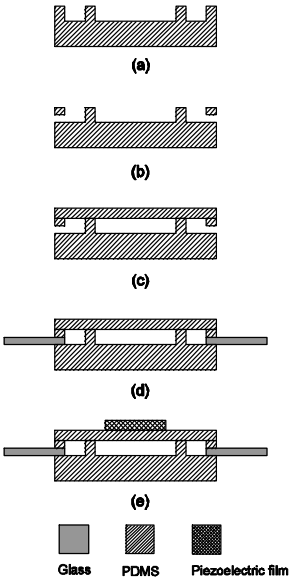

Fig. 7. Assembly steps of the energy harvester.

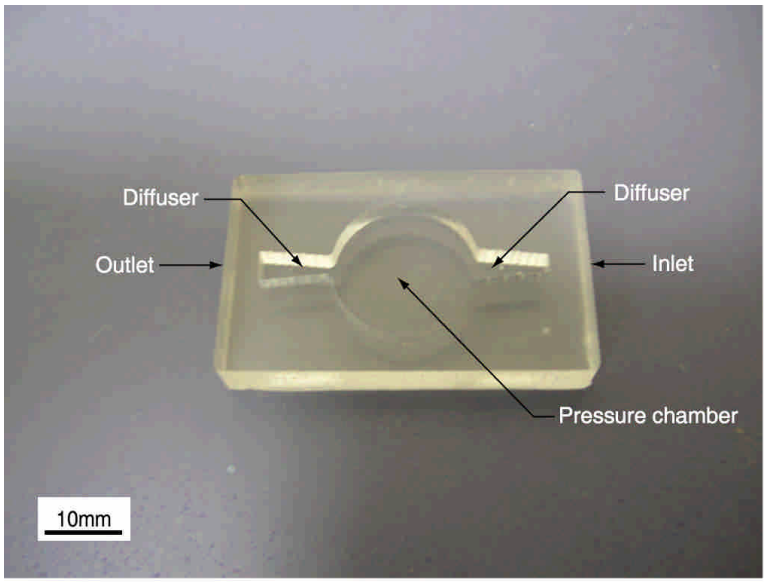

(a)

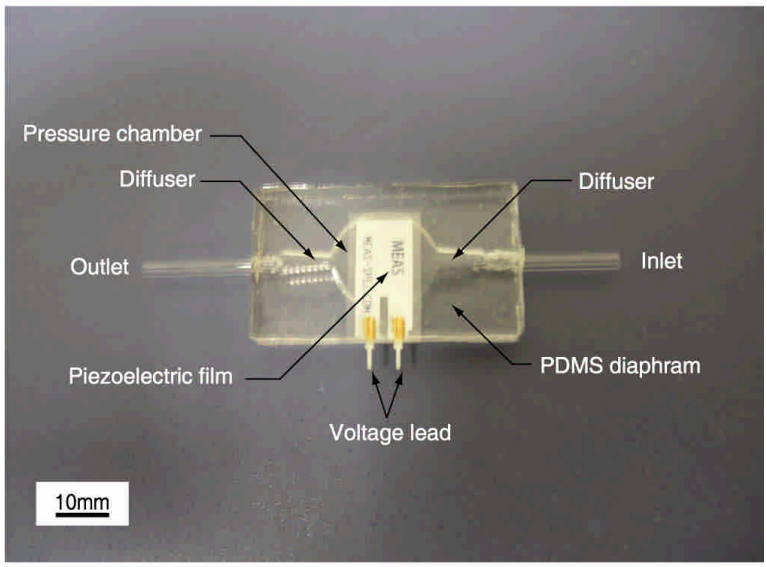

(b)

Fig. 8. (a) Fabricated PDMS channel. (b) Assembled energy harvester.

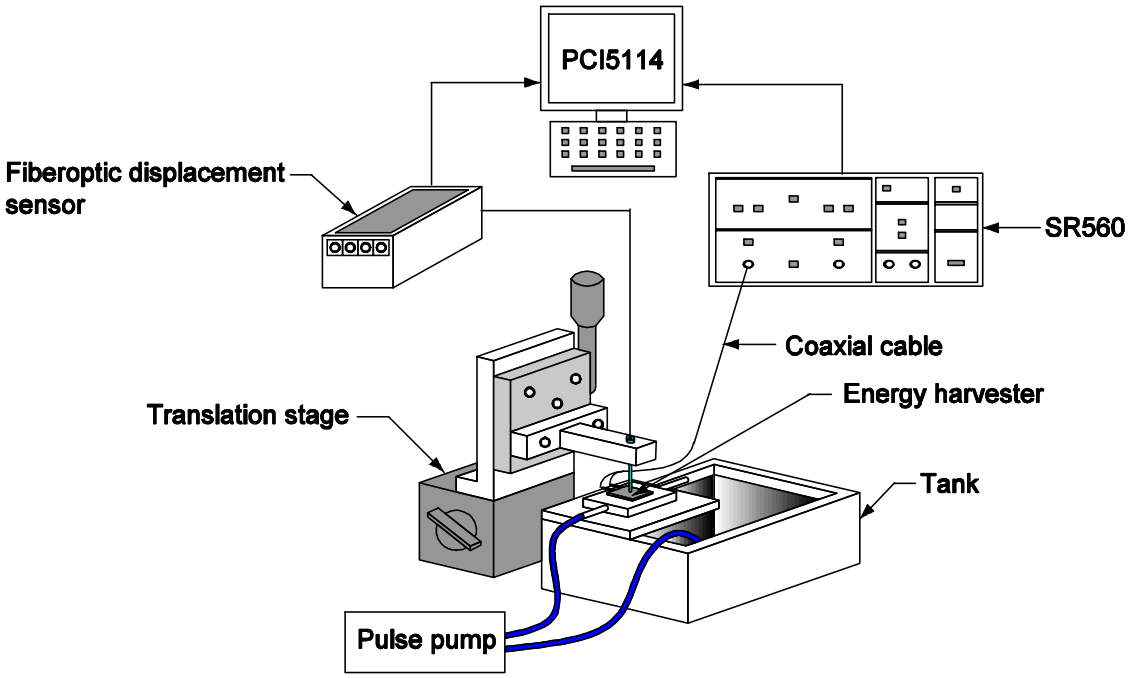

Fig. 9. Schematic of the experimental apparatus.

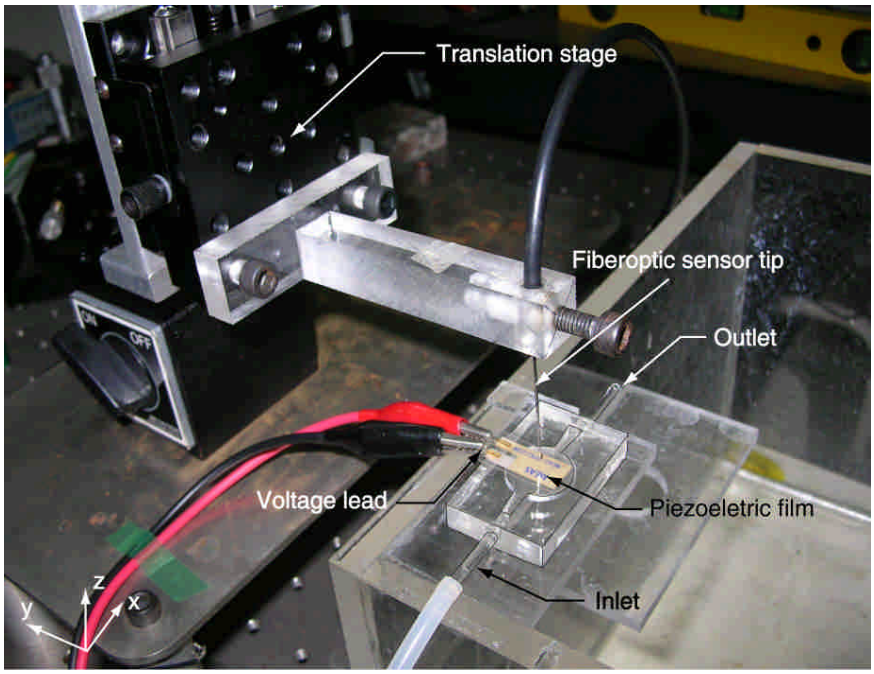

Fig. 10. Close-up view of the experimental apparatus.

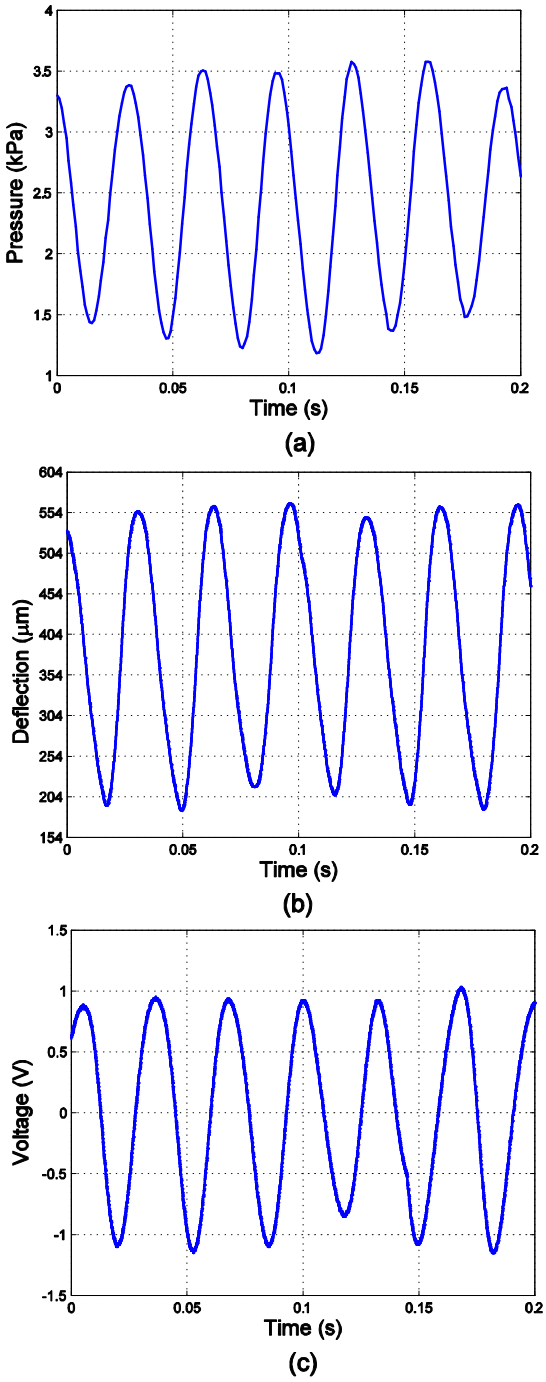

Fig. 11. Experimental results. (a) Pressure variation in the pressure chamber. (b) Deflection of the center of the piezoelectric film. (c) Output voltage of the PVDF film.

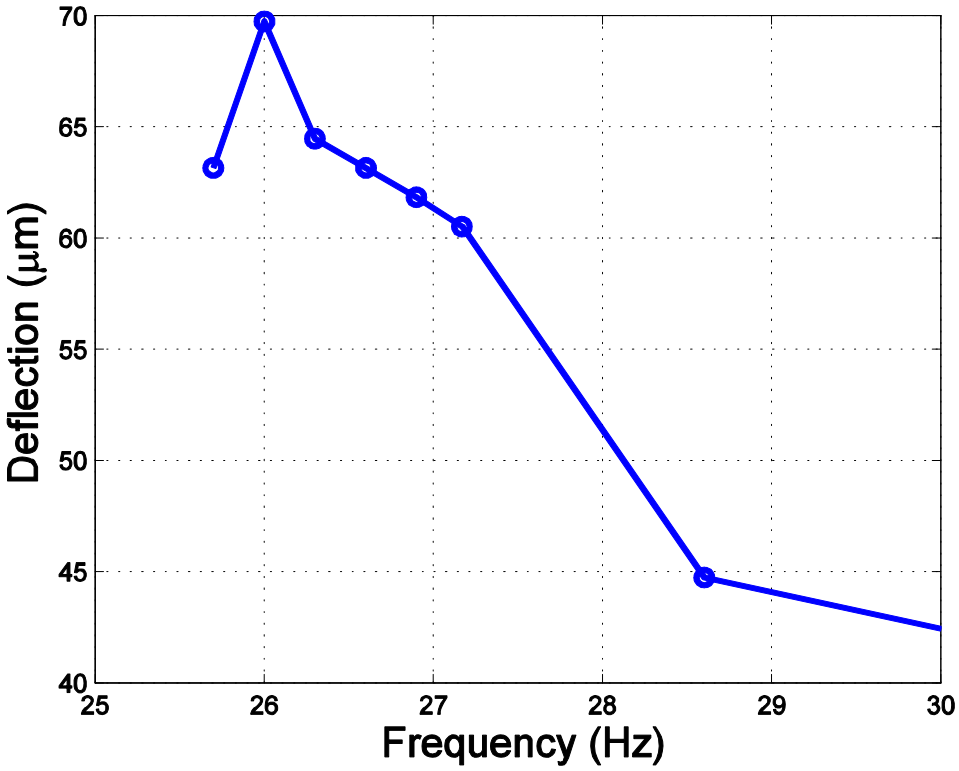

Fig. 12. The deflection of the center of the piezoelectric film as a function of the excitation frequency based on the experiments.